Genesis of tropical cyclone Nargis revealed by multiple satellite observations

Kazuyoshi Kikuchi,[1] Bin Wang,[1,2] and Hironori Fudeyasu[1]

Received 16 January 2009; accepted 26 February 2009; published 27 March 2009.

[1] Tropical cyclone (TC) Nargis recently battered Myanmar on May 2 2008 is one of the most deadly tropical storms in history. Nargis was initiated by an abnormally strong intraseasonal westerly event associated with Madden-Julian oscillation (MJO) in the eastern Indian Ocean. An incipient cyclonic disturbance emerged as an emanation of Rossby wave-induced vortex when the intraseasonal convective anomaly reached the Maritime Continent. The northeastward movement of MJO convection facilitated further development of the disturbance. The incipient disturbance became a tropical disturbance (TD) with a central warm-core structure on April 26. The further development from the TD to TC formation on April 28 is characterized by two distinctive stages: a radial contraction followed by a rapid intensification. The processes responsible for contraction and rapid intensification are discussed by diagnosis of multiple satellite data. This proposed new scenario is instrumental for understanding how a major TC develops in the northern Indian Ocean. **Citation:** Kikuchi, K., B. Wang, and H. Fudeyasu (2009), Genesis of tropical cyclone Nargis revealed by multiple satellite observations, *Geophys. Res. Lett.*, *36*, L06811, doi:10.1029/2009GL037296.

1. Introduction

[2] TC Nargis, recently emerged in the northern Indian Ocean (NIO) and battered Myanmar on May 2, 2008 [e.g., *Lin et al.*, 2009], is one of the most deadly tropical storms. Over 130,000 fatalities have been reported. Given the dense population and inadequate infrastructures, devastating TCs are a major threat to the livelihood in Southeast Asia. Despite of this, the formation, development, and movement of TCs in the NIO have received little attention compared to those in the Pacific and Atlantic. Lack of observations over the NIO is one of the major reasons that have hindered advancement of our knowledge.

[3] While the general favorable environmental conditions are well known [e.g., *Briegel and Frank*, 1997], the TC genesis remains the least understood matter among TC issues due to insufficient *in situ* high resolution observation and the complex nature of multi-scale interactions [*Holland*, 1995]. It has been well recognized that TCs never arise spontaneously [*Emanuel*, 2003]. Incipient disturbances are often required in order to initiate a TD. Easterly waves are a major player in the Atlantic and eastern North Pacific TC genesis [e.g., *Landsea et al.*, 1998], and monsoon confluence zone and Rossby wave energy dispersion also play an important role over the western North Pacific [e.g., *Ritchie and Holland*, 1999]. The aforementioned incipient disturbances, however, are virtually absent in the NIO. Thus, initiation process of TD in the NIO is expected to be different from the aforementioned basins. Previous studies have documented how equatorial waves including MJO events provide favorable large scale conditions for TC generation [e.g., *Bessafi and Wheeler*, 2006; *Frank and Roundy*, 2006; *Zhou and Wang*, 2007]. The MJO and associated equatorial waves are most active over the equatorial Indian Ocean (IO). It is conceivable that some equatorial waves which have rotational component may contribute to TC genesis by changing environment and directly initiating TD.

[4] In this study, we examine how Nargis was initiated from an MJO event and evolved from a weak to a strong storm. Our strategy is to use as many available satellite data as possible to reveal evolution of dynamic and thermodynamic structures of Nargis.

2. Data, Methodology, and Terminology

[5] The following satellite data were used in our study: (1) daily outgoing longwave radiation (OLR) data for depicting organized convection; (2) pixel-resolution infrared (IR) brightness temperature data, globally-merged from all available geostationary satellites for depicting development of clouds; (3) Sea surface winds data obtained by blending multiple satellites including QuikSCAT, Special Sensor Microwave/Imagers, Tropical Rainfall Measuring Mission (TRMM) Microwave Imager (TMI), and Advanced Microwave Scanning Radiometer observations on a 0.25° grid and 6-hourly time resolution for describing near surface wind field; (4) Atmospheric Infrared Sounder (AIRS) version 5 swath data for describing three dimensional temperature structure; and (5) TRMM TMI SST data gridded with $0.25° \times 0.25°$.

[6] Nargis was detected as a deep depression on April 26 by the Indian Meteorological Department and as a tropical storm (TS) at 12Z 27 by Joint Typhoon Warning Center (JTWC). To depict the early history of the TC, we objectively determined the centers of TD disturbance by using the technique developed by *Kurihara et al.* [1995]. First, surface wind field was decomposed into a basic flow and a disturbance. The TD center was determined by optimization of the central location so that the maximum of the azimuthally mean tangential wind within 6° from the center is maximized. After reaching the TS stage when the JTWC best track data became available, the results derived from

[1]International Pacific Research Center, University of Hawaii, Honolulu, Hawaii, USA.
[2]College of Physical and Environmental Oceanography, Ocean University of China, Qingdao, China.

0094-8276/09/2009GL037296$05.00

Table 1. Tropical Cyclone Classification

10-Minute Sustained Winds (Knots)	Atlantic and ENP/WNP	NIO
∼28	Tropical depression	Depression
28∼33	Tropical depression	Deep depression
34∼47	Tropical storm	Cyclonic storm
48∼63	Tropical storm	Severe cyclonic storm
64∼119	Hurricane/Typhoon	Very severe cyclonic storm
120∼	Hurricane/Typhoon	Super cyclonic storm

the technique explained above are similar to those from the best track. Thus, the satellite-observed surface winds allow us detect initiation process a few days ahead of TS formation.

[7] For classification of TC intensity, we use the terminology that is commonly used for Hurricanes and Typhoons in the Atlantic and Pacific Oceans to facilitate comparison (Table 1). We categorize TC development as the following stages: (i) pre-TD, (ii) TD, (iii) TS, and (iv) hurricane.

3. Initiation of Nargis

[8] The TC Nargis formed in April 28, 2008, which is in the pre-TC season. The TC formation in the NIO exhibits double peaks in October–November and May–June (Figure 1a), which correspond to the transitional season when equatorial westerly prevails. Historically, the likelihood for a TC occurring in April is smaller than 14%. Why does such a strong TC Nargis forms in April? What we found is that although climatologically the equatorial IO has not entered a westerly regime, a notable lasting abnormally strong westerly event had occurred in the mid-late April, lasting for about 10 days from April 16 to April 26 (Figure 1b). It was this westerly event that played a critical role in initiation of the Nargis. The westerly event was accompanied by organized convections. Both moved eastward slowly at a speed about 6 m s^{-1}. Those characteristics are consistent with well-known MJO.

[9] On April 21 when the intraseasonal westerly event reaches its peak. Two off-equatorial vortices associated with the equatorial westerly anomalies were first formed in the southeastern IO (Figure 2a), while NIO has no vortex formed and only a cloud cluster was seen. The early development of off-equatorial vortices in the southern hemisphere is attributed to the effect of the strong low-level background cyclonic shear due to the southeast trades and the equatorial westerly. In the ensuing two days, the organized convections shifted eastward a little bit and the major body reached the Maritime Continent (MC), when a weak cyclonic circulation emerged as an emanated Rossby wave vortex [*Kemball-Cook and Wang*, 2001] near the northwest tip of Sumatera Island on 12Z April 23 (Figure 2b). From April 23 to 25, the northeastward movement of the convections facilitated the development of the embedded incipient disturbance near Sumatera developed into a well defined TD on 12Z April 25 (Figure 2c). At the same time, the convections associated with southern hemisphere vortices continuously weakened. From April 25 to 27, the northern vortex moved northwestward and its cyclonic circulation dominated entire Bay of Bengal (BOB) (Figure 2d), which eventually developed into the Hurricane-strength Nargis on 06Z April 28.

[10] The northeastward shift of the MJO convection in the equatorial IO, which is critical for initiation of Nargis, is a common feature of boreal summer MJO [e.g., *Kemball-Cook and Wang*, 2001]. The northeastward movement of MJO has been attributed to atmosphere-ocean interaction [*Fu et al.*, 2003]. The northward migration of cyclonic vortex in the BOB is probably due to the effect of the environmental easterly vertical shear [*Jiang et al.*, 2004] and the northward SST gradient as shown in Figure 3a. The easterly vertical shear is also a favorable condition for cyclonic develop [*Wang and Xie*, 1996].

[11] The northward movement of the pre-TD disturbance may contribute to establishment of a TD in the early stage. From April 23 to 25, the planetary vorticity became 1.4 times larger due to the northward movement from 5°N to 7°N (Figure 3a). As relative vorticity is generated by absolute vorticity multiplied by divergence, the generation of relative vorticity by convergent flow becomes more effective, even for the same amount of the Ekman pumping.

4. Formation Processes of Nargis

[12] Here we document how the TD initiated by the MJO event developed and turned into Hurricane-strength Nargis.

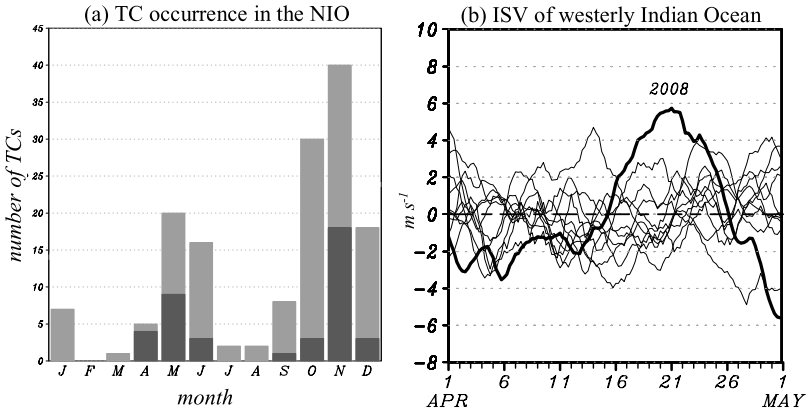

Figure 1. (a) Accumulated number of occurrence of TCs (dark), and TCs and TSs (light) during 1979–2007 as a function of month. (b) Westerly wind burst index defined by averaged zonal wind speed (5°S–5°N, 80°E–100°E). The thick line shows 2008 case and other thin lines indicate cases of 1998–2007. Five day running mean was taken and monthly mean was subtracted.

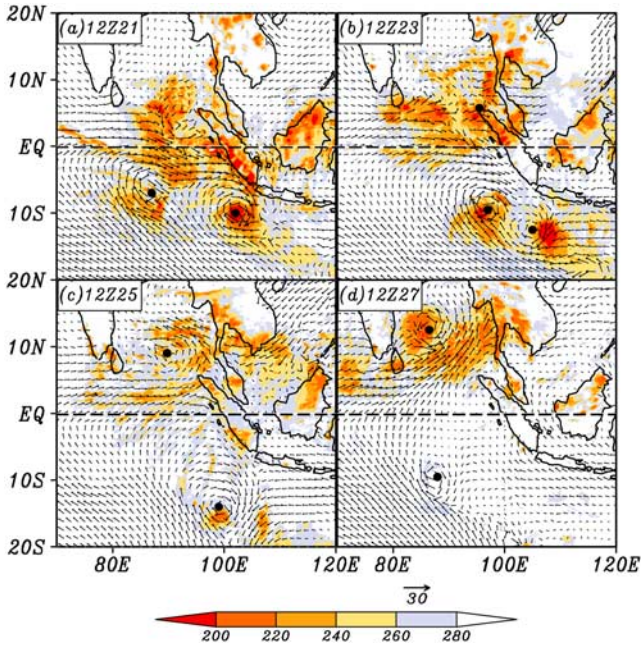

Figure 2. Temporal evolution of incipient disturbance and tropical depressions. Blended sea surface winds are indicated by vectors and infrared (IR) brightness temperature by shades (K). Closed circles represent votex centers deduced from the surface winds.

Figure 3b shows time evolutions of satellite-derived maximum surface wind speed (MW), number of deep convection pixels (indication of precipitation), and the radius of maximum winds (RMW) from April 23 (pre-TD) to April 30 (Hurricane). Note that the MW derived from satellite observation and the best track estimation show consistent temporal evolution but with different amplitude due to different derivation methods and criteria. As discussed in section 2, the TC development was categorized into four stages.

[13] Contraction is a salient process throughout the TD and TS stages, which fills the structural gap between the incipient TD and mature TC. A key responsible for contraction may be an interaction between convection and synoptic dynamics of TD. On its earlier development stage, organized convections were found to the north–west and -east of the TD center by about 200–300 km away (Figure 4a) which corresponds to RMW value at around this time (Figure 3b). Indeed, the relationship between strong surface winds and active convection was robust even in the early TD stage (Figure 5a). AIRS observation is luckily available which gives an important evidence that warming occurs in the places just around active convective areas, especially around the TD center (Figure 4a). Note that the temperature in deep convective areas cannot be retrieved with fidelity and thus missing here, but under partial cloud cover it can be retrieved with RMS errors on the order of, or less than, 1°K in 1-km-thick layer from the surface to 300 mb [*Susskind et al.*, 2003]. The warming results in a *warm core* structure (~3 K), which can be clearly seen in the horizontal-vertical profile of temperature anomaly (Figure 4b). The formation of the warm core at this early stage is important in spinning-up the TD by lowering surface pressure at the TD center. During this stage, northward migration (Figure 3a) is also favorable for enhancing convection by enhancing boundary layer convergence due to increase of the Coriolis parameter.

[14] As RMW reduced to ~200 km, the MW started to intensify dramatically. In the 24 hours starting from 12Z April 27 the MW increased from 17 m s^{-1} to 33 m s^{-1}, becoming a Hurricane (Figure 3b). This qualified as a rapid intensification [*Kaplan and DeMaria*, 2003].

[15] An interesting feature to note is that the interaction between convection and circulation shows odd correspondence in the rapid intensification. While MW increased rather monotonously, deep convection suddenly dropped around 06Z April 28 after rapid development. The key process responsible for this may be related to the structural change of TD. Axisymmetry seems to become more evident in the later rapid intensification period (Figures 5b–5d). To check this hypothesis, we define "symmetricity" by K_E^s/K_E^t.

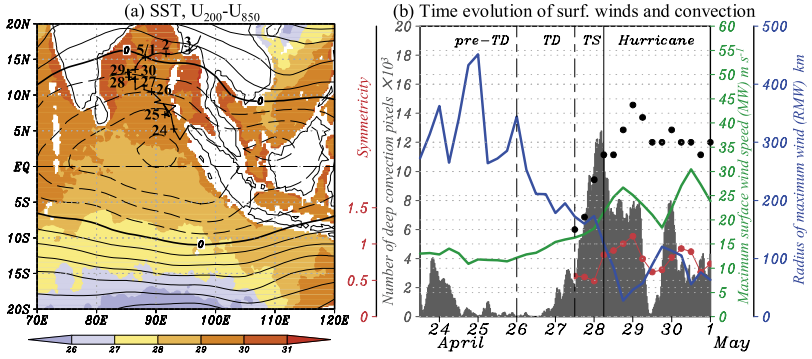

Figure 3. (a) Background SST (shades, °C) and zonal wind vertical shear between 200 and 850 hPa (contours) from NCEP/NCAR reanalysis averaged for the period April 23–May 1 2008. Positive vertical shear (denoted by solid contours) means westerly vertical shear and the contour interval is 5 m s^{-1}. The thick solid segments indicate the track of the pre-TD, TD, TS, and Hurricane. The numbers nearby indicate dates. (b) Time evolution of deep convection (IR ≤ 200 K) population (bar) within 400 km, maximum surface wind speed (green line), the radius of maximum wind (blue line), and the symmetricity of surface winds averaged within 300 km (red line) with reference to the pre-TD, TD, TS, or Hurricane centers. Closed circles are 1-minute mean sustained 10-m wind speed provided by JTWC. Three point average was taken for MW and RMW (thick lines).

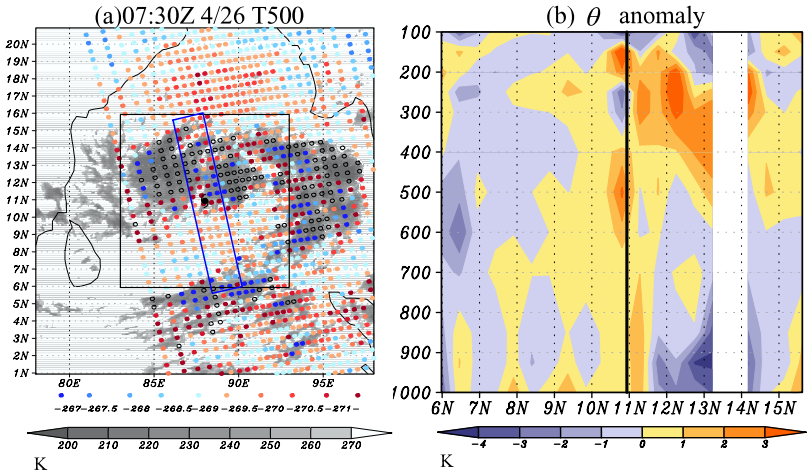

Figure 4. AIRS observation of (a) temperature at 500 hPa (circles) around 0730UTC, April 26 2008 together with IR at 0730UTC, April 26 (shades). The weather symbol represents the TD center. The black rectangle indicates 10° × 10° box centered on the TD center. The blue box indicates the area that were used to make the composite Figure 4b. (b) Horizontal-vertical distribution of potential temperature anomaly deviated from the black rectangle area in Figure 4a. Average was taken up to four footprints along each scan shown in Figure 4a. X axis indicates average latitude over the four footprints and the center location of the TD is shown by the thick line.

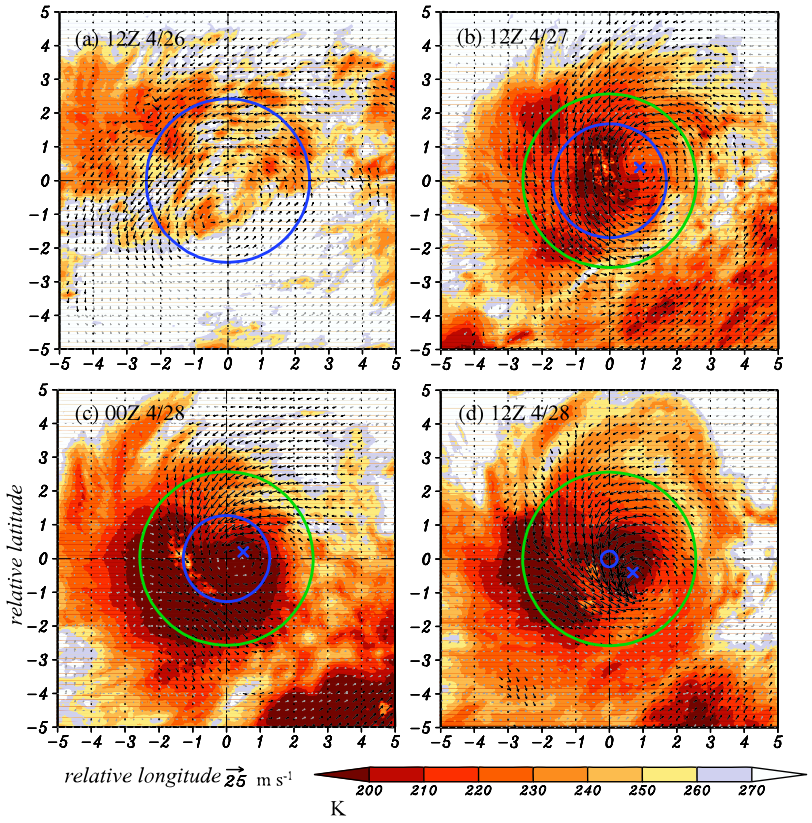

Figure 5. Horizontal distribution of IR (shades in units of K) and surface winds of disturbance component (vectors) around the pre-TD, TD, TS, or Hurricane center. The center location (0°, 0°) provided by JTWC was used after it became available on 12Z April 27. The center locations estimated by *Kurihara et al.*'s [1995] method are indicated by × for comparison. Surface wind speed less than or equal to 6 m s^{-1} are represented by gray arrows and greater than 6 m s^{-1} by black arrows. The blue circles represent radius of maximum wind, and the green circles 300 km radius from the center.

Where $K_E^s(r, \theta)$ and $K_E^t(r)$ are axisymmetric component of and total kinetic energy of surface winds, respectively, expressed in terms of the TC-centered cylindrical coordinate system (r, θ). After all, the time evolution of the symmetricity appears to support our hypothesis (Figure 3b). The feature of axisymmetrization characterized by outward propagating asymmetric component of both IR and surface winds (Figure 5) is consistent with the theoretical work by *Montgomery and Enagonio* [1998] that showed the warm core reinforcement occurs as a result of axisymmetrization. Note that the aforementioned conclusion is the same no matter how the center location is determined (JTWC or *Kurihara et al.*'s [1995], Figure 5).

5. Discussion and Summary

[16] By examining multiple satellite observations, a new scenario of how Nargis was initiated and formed in the pre-TC season in the NIO was proposed. First, an abnormally strong intraseasonal westerly occurred in mid-late April which is associated with MJO and accompanied by organized convections. When the main body of the convections reached the MC, the pre-TD disturbance was initiated as an emanated Rossby wave vortex near the northern tip of Sumatera on April 23, 2008. The northeastward movement of organized convection associated with MJO facilitated further development of the pre-TD. Once the pre-TD developed to some extent, the strong connection between well-built surface winds and active convection made it possible to create a warm core structure in its center, forming the TD on April 26. The middle tropospheric warming near the TD center lowers surface pressure, resulting in contraction of the band of maximum winds and convection. The continuous northward migration may further strengthen the pre-TD disturbance and the TD by increasing boundary layer convergence due to the increase of the Coriolis parameter. As contraction reaches a certain threshold, the cooperation between convection and synoptic dynamics of TD was accelerated, resulting in rapid intensification and turning into a hurricane in the end. Two stages were involved in the rapid intensification, i) deep convection development with strong axial asymmetry and ii) axisymmetrization process.

[17] The present study has not only presented a timely and concise analysis of one of the most disastrous weather event worldwide in 2008, but also provided a new perspective on the TC genesis process in the NIO. While the proposed scenario seems to be reasonable, other factors have not been well examined due to limitation of satellite data availability. To achieve a more comprehensible understanding, a number of issues such as the effects of the steering flow and beta drift on the movement and vertical shear on the development need to be further clarified.

[18] **Acknowledgments.** This research was supported by ONR grant N00014-02-0532. Additional support was provided by the Japan Agency for Marine-Earth Science and Technology (JAMSTEC), by NASA through grant NNX07AG53G, and by NOAA through grant NA17RJ1230 through their sponsorship of research activities at the International Pacific Research Center. The blended surface wind data are acquired from NOAA's NCDC, via their website http://www.ncdc.noaa.gov/oa/rsad/blendedseawinds.html. We thank two anonymous reviewers for their insightful comments. This manuscript is SOEST contribution 7633 and IPRC contribution 585.

References

Bessafi, M., and M. C. Wheeler (2006), Modulation of south Indian Ocean tropical cyclones by the Madden-Julian oscillation and convectively coupled equatorial waves, *Mon. Weather Rev.*, *134*, 638–656.

Briegel, L. M., and W. M. Frank (1997), Large-scale influences on tropical cyclogenesis in the western North Pacific, *Mon. Weather Rev.*, *125*, 1397–1413.

Emanuel, K. (2003), Tropical cyclones, *Annu. Rev. Earth Sci.*, *31*, 75–104.

Frank, W. M., and P. E. Roundy (2006), The role of tropical waves in tropical cyclogenesis, *Mon. Weather Rev.*, *134*, 2397–2417.

Fu, X., B. Wang, T. Li, and J. P. McCreary (2003), Coupling between northward-propagating, intraseasonal oscillations and sea surface temperature in the Indian Ocean, *J. Atmos. Sci.*, *60*, 1733–1753.

Holland, G. J. (1995), Scale interaction in the western Pacific monsoon, *Meteorol. Atmos. Phys.*, *56*, 57–79.

Jiang, X., T. Li, and B. Wang (2004), Structures and mechanisms of the northward propagating boreal summer intraseasonal oscillation, *J. Clim.*, *17*, 1022–1039.

Kaplan, J., and M. DeMaria (2003), Large-scale characteristics of rapidly intensifying tropical cyclones in the North Atlantic basin, *Weather Forecast.*, *18*, 1093–1108.

Kemball-Cook, S., and B. Wang (2001), Equatorial waves and air-sea interaction in the boreal summer intraseasonal oscillation, *J. Clim.*, *14*, 2923–2942.

Kurihara, Y., M. A. Bender, R. E. Tuleya, and R. J. Ross (1995), Improvements in the GFDL hurricane prediction system, *Mon. Weather Rev.*, *123*, 2791–2801.

Landsea, C. W., G. D. Bell, W. M. Gray, and S. B. Goldenberg (1998), The extremely active 1995 Atlantic hurricane season: Environmental conditions and verification of seasonal forecasts, *Mon. Weather Rev.*, *126*, 1174–1193.

Lin, I.-I., C.-H. Chen, I.-F. Pun, W. T. Liu, and C.-C. Wu (2009), Warm ocean anomaly, air sea fluxes, and the rapid intensification of tropical cyclone Nargis, *Geophys. Res. Lett.*, *36*, L03817, doi:10.1029/2008GL035815.

Montgomery, M. T., and J. Enagonio (1998), Tropical cyclogenesis via convectively forced vortex Rossby waves in a three-dimensional quasi-geostrophic model, *J. Atmos. Sci.*, *55*, 3176–3207.

Ritchie, E. A., and G. J. Holland (1999), Large-scale patterns associated with tropical cyclogenesis in the western Pacific, *Mon. Weather Rev.*, *127*, 2027–2043.

Susskind, J., C. D. Barnet, and J. M. Blaisdell (2003), Retrieval of atmospheric and surface parameters from AIRS/AMSU/HSB data in the presence of clouds, *IEEE Trans. Geosci. Remote Sens.*, *41*, 390–409.

Wang, B., and X. Xie (1996), Low-frequency equatorial waves in vertically sheared zonal flow. Part I: Stable waves, *J. Atmos. Sci.*, *53*, 449–467.

Zhou, X. Q., and B. Wang (2007), Transition from an eastern Pacific upper-level mixed Rossby-gravity wave to a western Pacific tropical cyclone, *Geophys. Res. Lett.*, *34*, L24801, doi:10.1029/2007GL031831.

H. Fudeyasu, K. Kikuchi, and B. Wang, International Pacific Research Center, University of Hawaii, POST Building 401, 1680 East West Road, Honolulu, HI 96822, USA. (kazuyosh@hawaii.edu)